

## **Supplementary Data**

### **The DNA binding CXC domain of MSL2 is required for faithful targeting the Dosage Compensation Complex to the X chromosome**

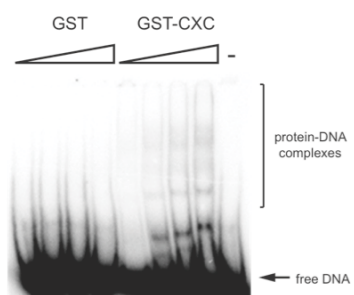
Torsten Fauth, Felix Mueller-Planitz, Cornelia König, Tobias Straub  
and Peter B. Becker

Adolf-Butenandt-Institute and Centre for Integrated Protein Science (CiPSM)

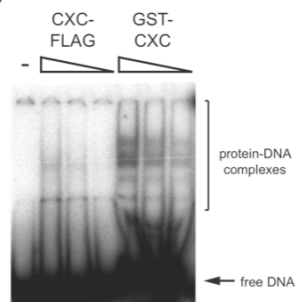
Ludwig-Maximilians-University, 80336 Munich, Germany.

Figure S1

A

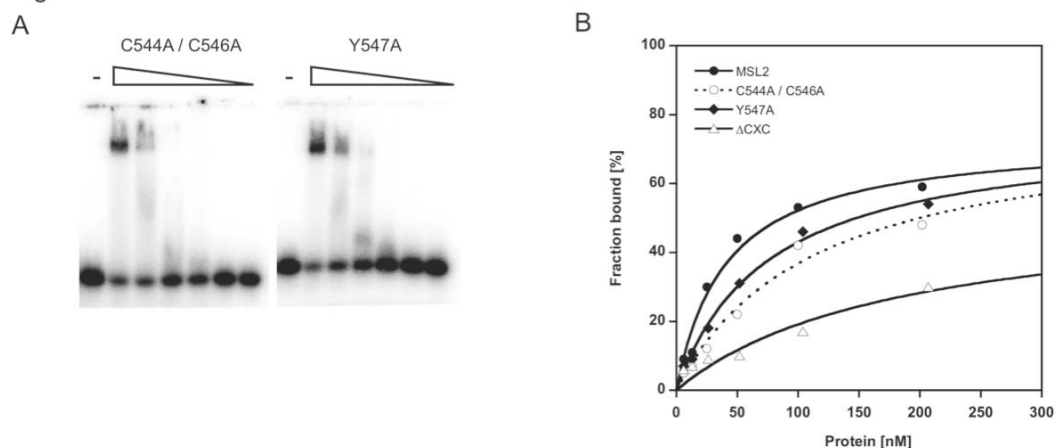


B



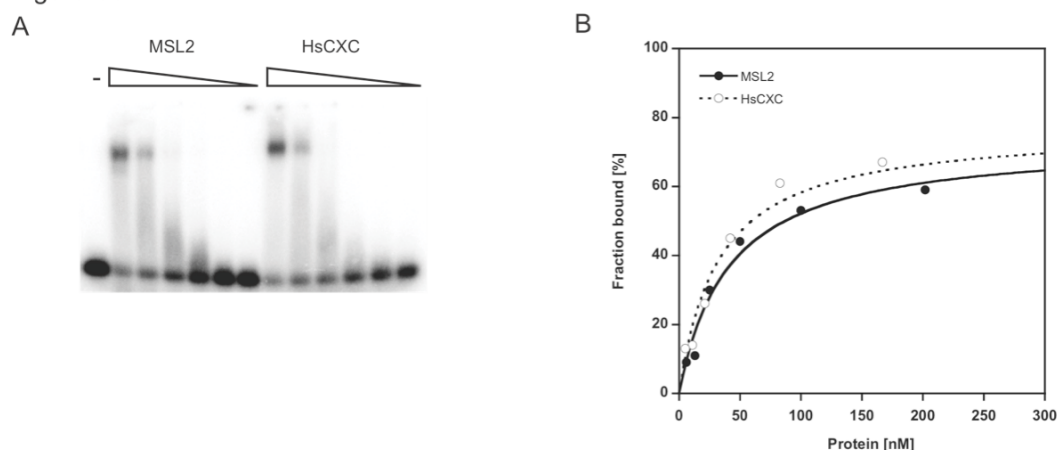
**Figure S1:** Binding of the isolated recombinant CXC domain to a DNA high affinity site *in vitro*. Increasing concentrations (1 - 8  $\mu\text{M}$ ) of (A) GST and GST-CXC or of (B) CXC-FLAG (5 - 20  $\mu\text{M}$ ) and GST-CXC (2 - 8  $\mu\text{M}$ ) were incubated with radiolabeled 40 bp DBF12-L15 dsDNA and protein-DNA complexes were separated from unbound DNA in non-denaturing polyacrylamide gels.

Figure S2



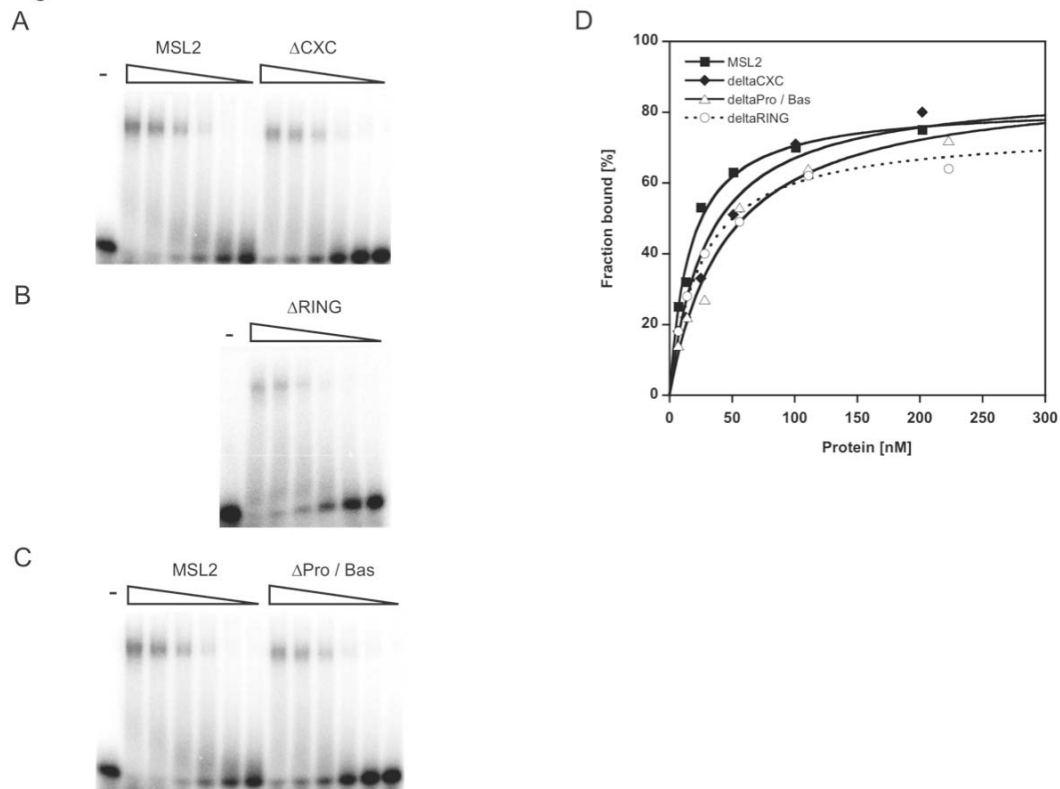
**Figure S2:** Binding of different recombinant MSL2 derivatives to a DNA high affinity site *in vitro*. Electrophoretic mobility shift assay. Increasing concentrations of MSL2 carrying point mutations in the CXC domain were incubated with radiolabeled 40 bp DBF12-L15 dsDNA and protein-DNA complexes were separated from unbound DNA in non-denaturing agarose gels. (B) Binding curves obtained from quantification of (A) and fitting to a standard bimolecular model. For comparison MSL2 $\Delta$ CXC is also displayed.

Figure S3



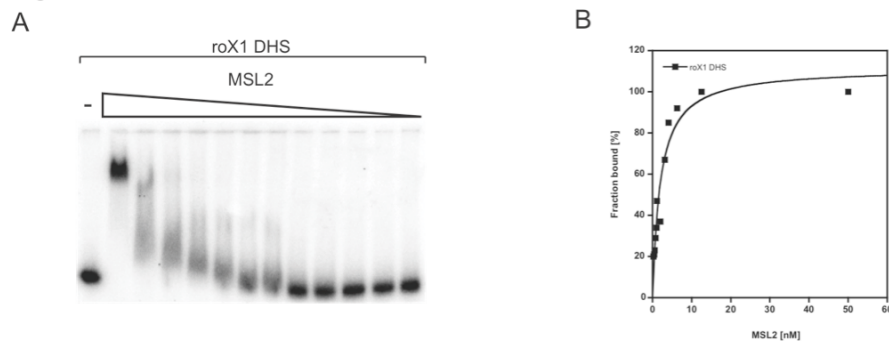
**Figure S3:** Binding of different recombinant MSL2 derivatives to a DNA high affinity site *in vitro*. Increasing concentrations of MSL2 and of the chimeric HsCXC were assayed as in Fig. S2.

Figure S4



**Figure S4:** Binding of different recombinant MSL2 derivatives to RNA. Electrophoretic mobility shift assays. Increasing concentrations of MSL2 and MSL2- $\Delta$ CXC (A), MSL2- $\Delta$ RING (B) or MSL2 and MSL2- $\Delta$ Pro/Bas (C) were incubated with radiolabeled dsRNA representing the DBF12-L15 sequence and protein-RNA complexes were separated from unbound RNA in non-denaturing agarose gels. (D) Binding curves obtained from quantification of EMSAs and fitting to a standard bimolecular model.

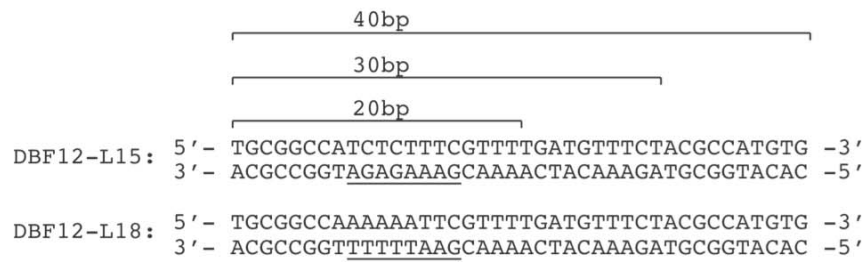
Figure S5



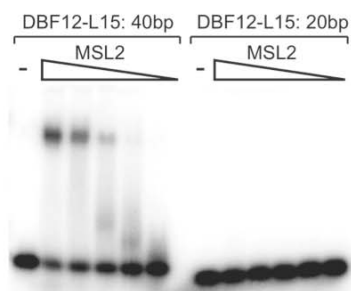
**Figure S5:** Binding of MSL2 to the HAS within the *roX1* gene *in vitro*. Electrophoretic mobility shift assays. (A) Increasing concentrations of MSL2 were incubated with radiolabeled 226 bp DNA fragment representing the HAS within the *roX1* gene (22) and protein-DNA complexes were separated from unbound DNA in non-denaturing agarose gels. (B) Binding curves obtained from quantification of (A) and fitting to a standard bimolecular model.

Figure S6

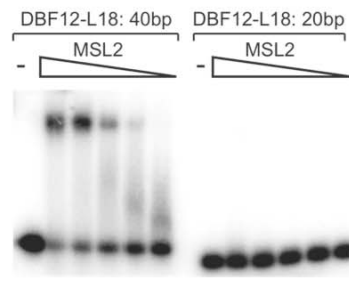
A



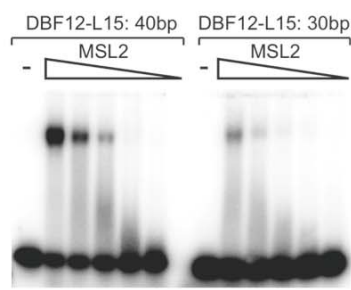
B



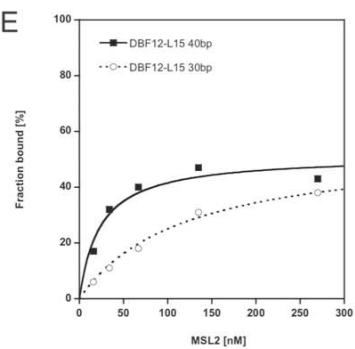
C



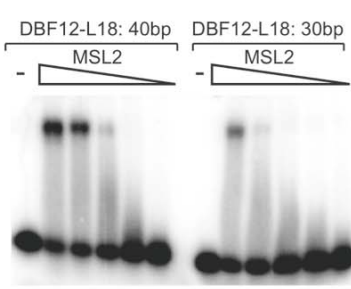
D



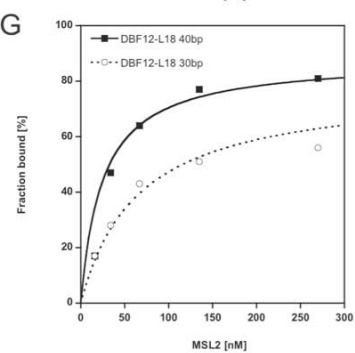
E



F



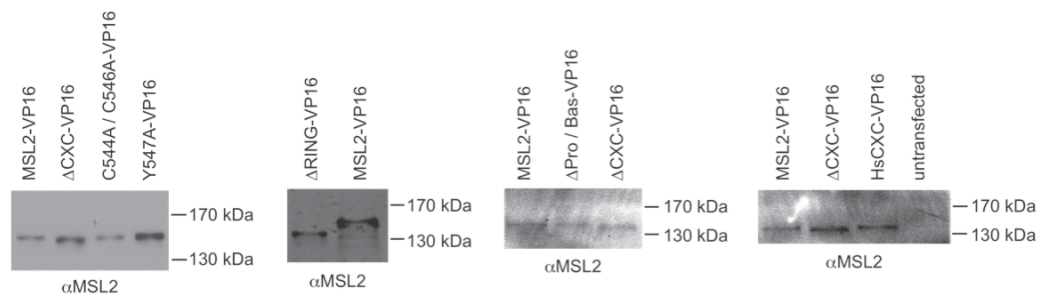
G



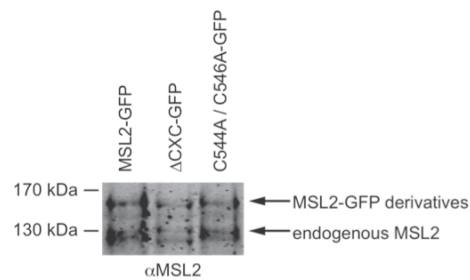
**Figure S6:** Binding of MSL2 to different DNA fragments *in vitro*. (A) Sequences of the DNA fragments used in EMSA. The GA-repeat of DBF12-L15 and the mutated sequence of DBF12-L18 are underlined. (B)-(G) Increasing concentrations of MSL2 were assayed as in Fig. S2.

Figure S7

A



B



**Figure S7:** Western blots showing expression of different MSL2 derivatives in SL2 cells. (A) Transiently transfected SL2 cells were harvested, lysed and proteins precipitated using TCA. Precipitated proteins from roughly  $2.5 \times 10^5$  cells were subjected to western blot analysis. (B) Stable SL2 cell lines were harvested, lysed and roughly  $5 \times 10^4$  cells were subjected to western blot analysis. A rabbit anti-MSL2 antibody was used to detect the endogenous and the different MSL2-GFP derivatives in all blots.